

## VASCULAR SYSTEM WITHIN DEVELOPING ROOT NODULES OF *LUPINUS LUTEUS* L. PART 2. DIFFERENTIATED NODULES\*\*

BARBARA ŁOTOCKA\*

Department of Botany, Warsaw University of Life Sciences,  
Nowoursynowska 159, 02-776 Warsaw, Poland

Received December 27, 2007; revision accepted February 20, 2008

The development and (ultra)structure of vascular tissue was studied in *Lupinus luteus* L. mature root nodules 25 and 60 days after inoculation. In the proximal part of the nodule vascular trace, extensive growth took place to match the secondary growth of the root. Development of bacteroid and vascular tissues was correlated. The non-anastomosing nodule vascular bundles elongated and branched due to the activity of nodule lateral meristems, thus forming an extensive vascular network within deep lobes of bacteroid tissue. The vascular trace and vascular bundles differed mainly in the location and ultrastructure of transfer cells and parenchymatous cells, in which the inner membrane of the nuclear envelope formed tubular invaginations within the dense chromatin. Development of the vascular system in the collar root nodule of lupine differed from that of cylindrical indeterminate nodules.

**Key words:** Cell nucleus, *Lupinus luteus* L., phloem, root nodule, transfer cells, vascular meristem, vascular tissue, xylem.

### INTRODUCTION

Years of interest in the symbiotic diazotrophy of legumes are reflected in many thousands of research papers available in public databases. Root nodule morphogenesis is an attractive experimental model for fundamental studies of plant development (Hirsch, 1992). Therefore it is surprising that among the thousands of papers related to the structure of the root nodules, just a few are devoted to its conductive tissue (Pate et al., 1969; Briarty, 1978).

In *Lupinus luteus* L. the root nodules are of indeterminate type but are very different from the typical cylindrical indeterminate nodules formed by legumes like *Pisum* sp., *Trifolium* sp. or *Medicago* sp. The anatomical differences between lupinoid and cylindrical indeterminate nodules result from differences in the mode of nodule initiation. In yellow lupine the nodule primordium is initiated in the sub-rhizodermal root cortex without the formation of an infection thread in the root hair, which is the microsymbiont's entry site (Łotocka et al., 2000a). During the subsequent juvenile stage in lupine root nodule formation, local dedifferentiation of primary root tissues

occurs and meristems are formed, which give rise to the three principal nodule tissue zones: protective, bacteroid and vascular (Łotocka et al., 2000a and Part 1 of the present work).

The present work addresses the developmental anatomy of the vascular system, which in *L. luteus* root nodules is especially extensive and complex. This part focuses on development of the vascular system in continuously growing mature nodules.

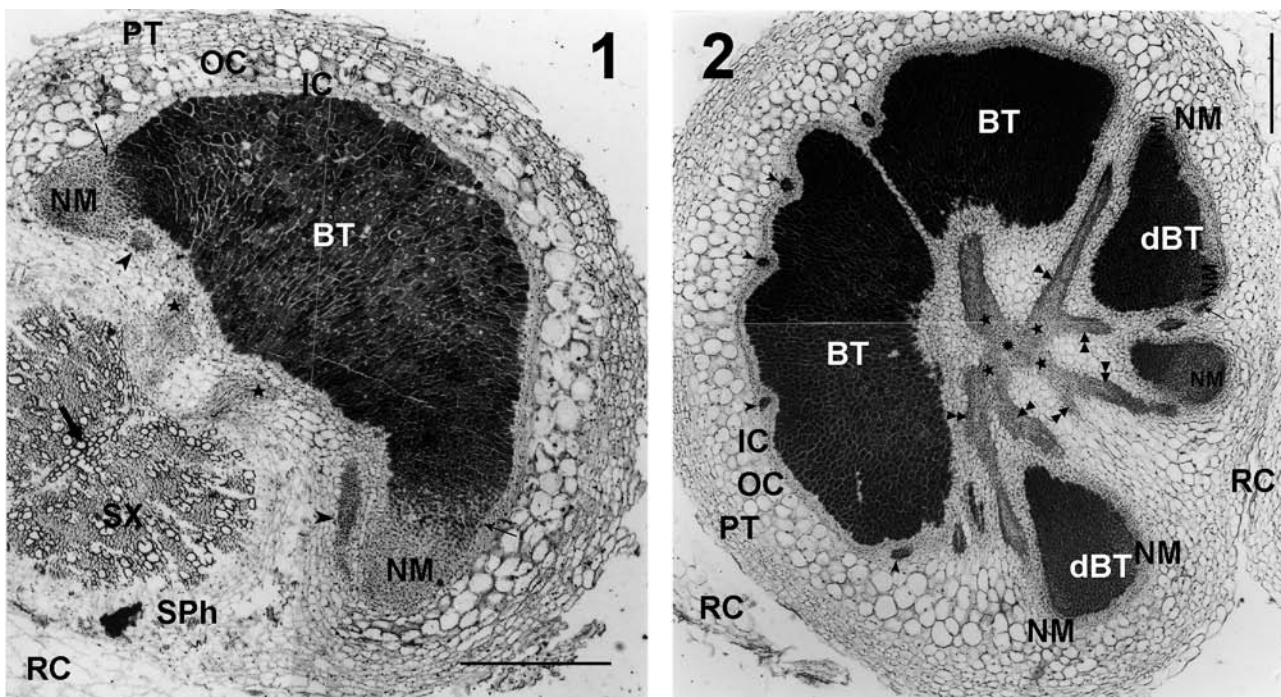
### MATERIALS AND METHODS

For microscopic study, three different stages of *Lupinus luteus* L. cv. Ventus nodule development were chosen. Two of them are reported in this work: the stage of full metabolic activity at 25 days after inoculation (DAI), and the 60 DAI stage, when a wide zone of senesced bacteroid tissue was present. The inoculation mode, plant growth conditions and bacterial or plant media were as described earlier (Łotocka et al., 2000b).

Only nodules from the upper part of the taproot initiated at a distance from other nodules were taken, to exclude nodules developmentally inhibited by neighboring ones. For resin embed-

\*e-mail: BŁotocka@gmail.com

\*\*This work is part of the author's unpublished doctoral dissertation



**Figs. 1, 2.** Root nodule of *Lupinus luteus* at fully differentiated stage, 25 DAI, sections transversal (Fig. 1) and tangential (Fig. 2) to root axis. BT – bacteroid tissue; dBT or thin arrows – differentiating bacteroid tissue; IC – inner cortex of nodule; NM – nodule meristem; OC – outer cortex of nodule; PT – protective tissue of nodule; RC – root cortex; SPh – secondary phloem; SX – secondary xylem; arrow – root protoxylem; stars – first-order ramifications of trace bundles in distal part; double arrowheads – second-order ramifications; arrowheads – third-order ramifications; rosette – position of NVT; double thin arrow – meristematic bundle tip at nodule meristem. Bars = 320  $\mu\text{m}$  in Fig. 1, 440  $\mu\text{m}$  in Fig. 2.

ment, nodules were dissected, and fragments containing the nodule vascular trace (NVT) or nodule vascular bundles (NVBs) were sampled separately. All samples for resin sections were processed identically, according to procedures described in Part 1 of this work. Samples were carefully positioned in embedment molds to ensure transversal, radial or tangential sectioning planes versus the root axis.

For paraffin sections, root fragments with intact root nodules were dehydrated in ethanol and xylene, embedded in paraffin wax, serial-sectioned transversely, radially or tangentially at 8–20  $\mu\text{m}$  thickness (depending on nodule size), and stained with Mayer's hematoxylin (Gerlach, 1972) to observe the location of dividing cells, or safranin/fast green (Broda, 1971) for general anatomy.

Samples containing NVT or NVBs from root nodules were macerated for 24 h according to Broda (1971) and carefully washed with distilled water; squash preparations mounted in glycerol were made for determination of tracheary element type.

Observations were made with light or transmission electron microscopes, as described in Part 1 of this work.

## RESULTS

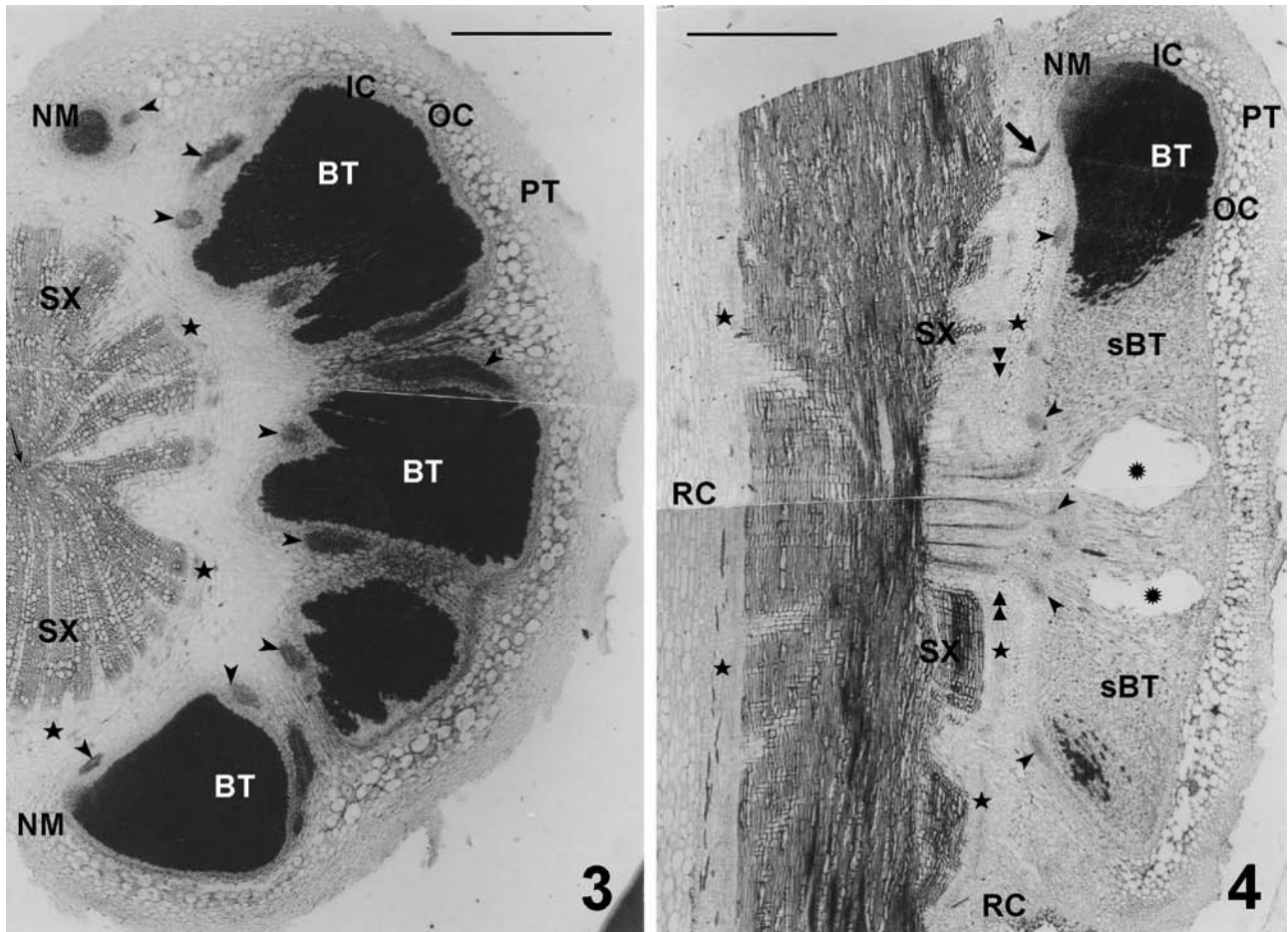
### PLANT DEVELOPMENT IN RELATION TO NODULATION

By 25 DAI the plants formed the 8<sup>th</sup> or 9<sup>th</sup> leaf and the upper several centimeters of taproot were covered with root nodules a few millimeters in diameter and intensely pink inside. By 60 DAI the plants formed the 21<sup>st</sup>–23<sup>rd</sup> leaf and were in full bloom. The oldest root nodules, which developed at a distance from the other ones and thus reached the maximum size possible, were ~10 mm in diameter, and their bacteroid tissue was intensely pink in its peripheral parts, and greenish and empty in central parts. Many root nodules were tightly clustered and intertwined.

### GENERAL ANATOMY OF ROOT NODULE

In nodules 25 DAI, tissues reached their fully differentiated form (Fig. 1). The bacteroid tissue took the form of a crescent in transversal section, and a shallowly lobed circle in tangential section. It was zonated into several lateral meristems at the proximal





**Figs. 3, 4.** Root nodule of *Lupinus luteus* with senesced zone present, 60 DAI, sections transversal (Fig. 3) and radial (Fig. 4) to root axis. BT – bacteroid tissue; IC – inner cortex of nodule; NM – nodule meristem; OC – outer cortex of nodule; PT – protective tissue of nodule; RC – root cortex; sBT – senescent bacteroid tissue; SX – secondary xylem; thin arrow – root primary xylem; stars – root secondary phloem; arrowheads – NVBs; double arrowheads indicate the height of NVT with several groups of trace bundles; arrow – single vascular bundle formed outside the NVT that connected the root secondary vascular tissues and root nodule; rosettes – empty space within degraded bacteroid tissue. Bars = 1050  $\mu$ m in Fig. 3, 1180  $\mu$ m in Fig. 4.

side of the tissue, differentiating bacteroid tissue and already differentiated bacteroid tissue. First-order ramifications of the nodule vascular trace (NVT), which during the juvenile stage were still immature, were differentiated in 25-day-old nodules, and the second- and some third-order branchings, that is, nodule vascular bundles (NVBs), were already formed (Fig. 2) at the proximal side of the bacteroid tissue. The NVBs formed meridians around the bacteroid tissue. Serial tangential sections showed that the bundles did not anastomose, but were ramified. The NVBs were separated from bacteroid tissue by biseriate inner cortex and uniseriate bundle endodermis.

The general anatomical organization of 60-day-old root nodules resembled that of 25-day-old ones. The bacteroid tissue still contained meristematic

zones, which were narrow and located laterally at the proximal side of bacteroid tissue lobes (Figs. 3, 4). The bacteroid tissue was divided into numerous lobes separated by cortical tissue (Figs. 3, 5), which contained numerous NVBs in every section. In the oldest bacteroid tissue, a new zone of completely degraded cells appeared, sometimes empty (Figs. 4, 5). The degraded region adjoined the distal NVT and its first- or second-order ramifications (cf. Figs. 2, 5). Nodule development between 25 and 60 DAI could be reconstructed from the anatomy of 60-day-old ones. For example, the oldest part of the degraded zone, marked with a dashed line in Fig. 5, corresponded to the cross-sectional outline of bacteroid tissue in 25-day-old nodules. Of six lateral meristems then present in this particular nodule, only two continued growth. One of them divided once subsequently and

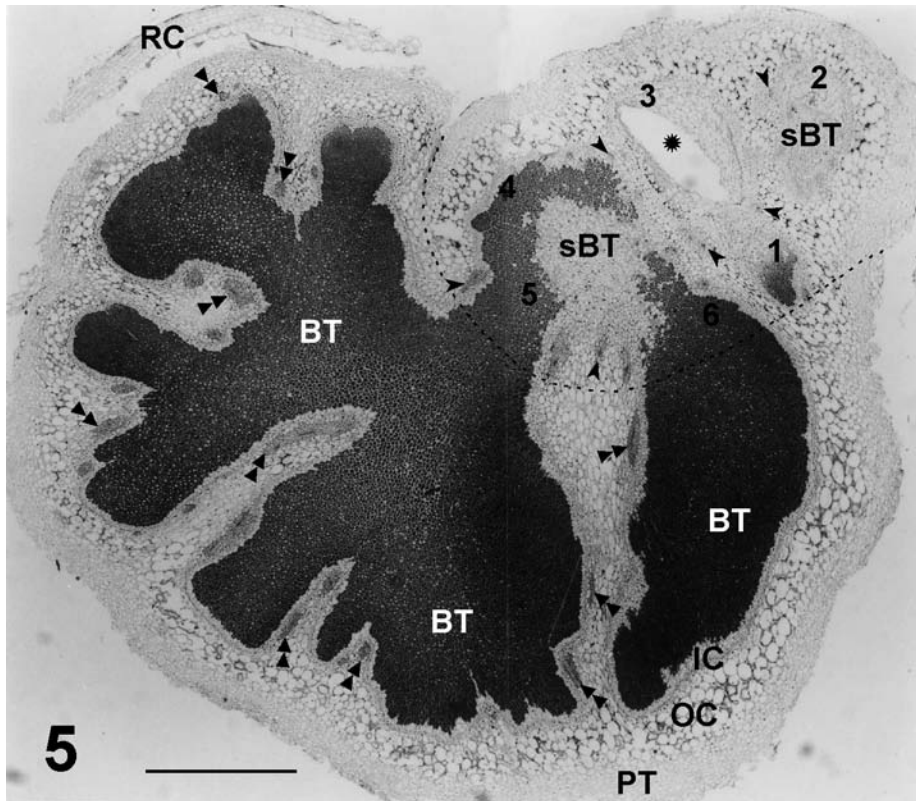


**Fig. 5.** Root nodule of *Lupinus luteus* with senesced zone present, 60 DAI, section tangential to root axis. BT – bacteroid tissue; IC – inner cortex of nodule; OC – outer cortex of nodule; PT – protective tissue of nodule; RC – root cortex; sBT – senescent bacteroid tissue; dashed line – putative outline of bacteroid tissue tangential section in 25-day-old nodule; 1–6 – putative positions of meristems in 25-day-old nodule (note that only two maintained growth); arrowheads – first- and second-order ramifications of NVT; double arrowheads – finer ramifications; rosette – empty space within degraded bacteroid tissue. Bar = 1180  $\mu$ m.

produced a compact region of bacteroid tissue; the other underwent several divisions and formed most of the bacteroid tissue lobes that were functional at the time of fixation. The part of the nodule that developed most intensely grew towards a space on the tap-root devoid of nodules; another nodule was present near the side of the developmentally blocked and mostly degraded bacteroid tissue.

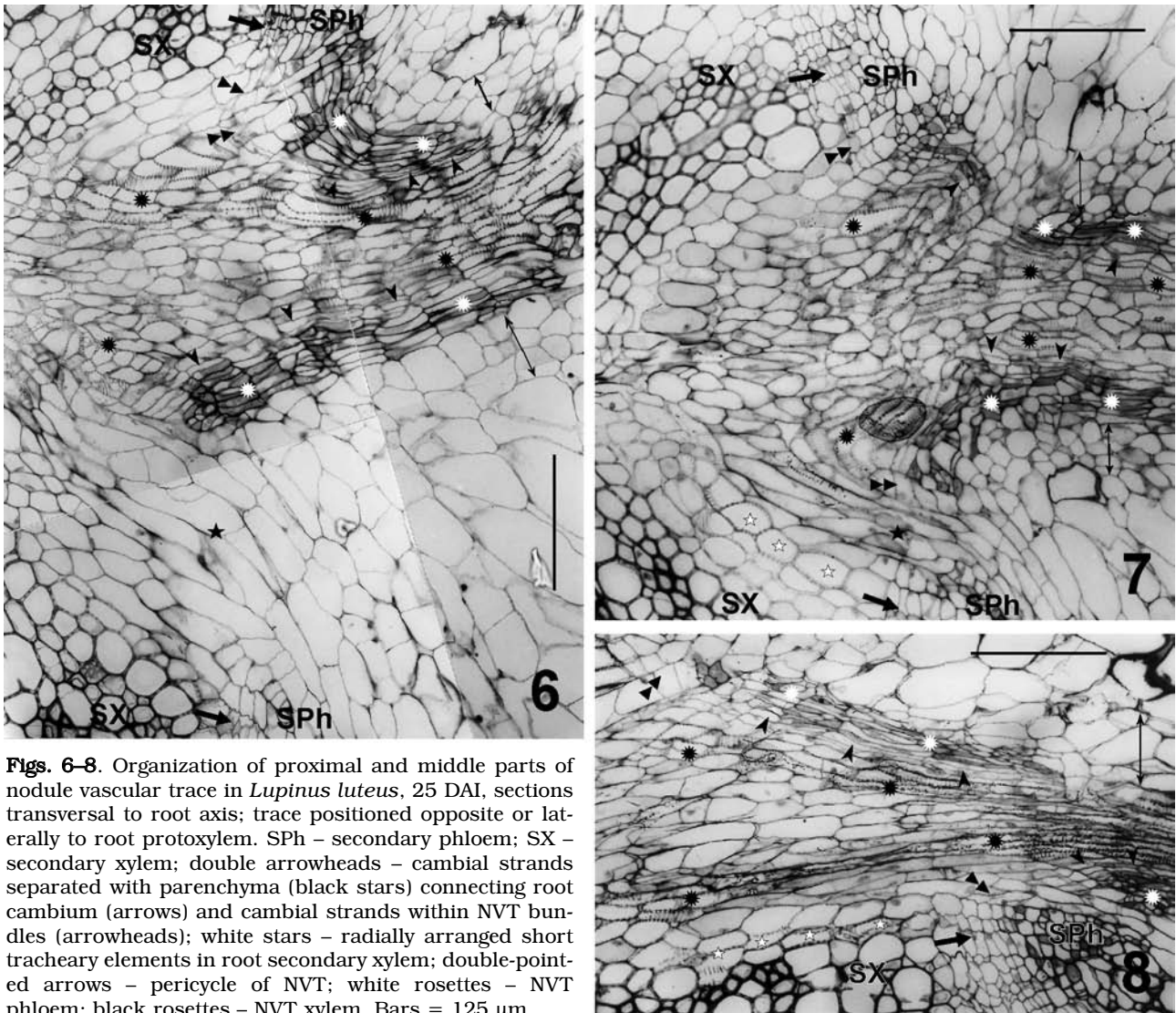
#### NODULE VASCULAR TRACE – ANATOMY

The organization of the NVT was analyzed in transversal, radial and tangential semi-thin sections of nodulated root. Transversal serial sections showed that the otherwise narrow parenchymatous ray, which in the non-inoculated root adjoined the protoxylem, was widened within the root nodule 25 DAI due to the development of the proximal part of the NVT (Figs. 6, 7, 10, 11). Characteristically, the vessels of root secondary xylem at the margin of that ray were short and radial rather than axial (Figs. 7, 8). Depending on the location of bacteroid tissue initials (BTI) versus the protoxylem, which determined

the direction of NVT formation, the trace was positioned centrally within the ray (BTI exactly opposite protoxylem; Fig. 7), or else it differentiated at its left or right side (Figs. 6 or 8, respectively; BTI located laterally versus protoxylem). In some nodules the trace's bundles occurred in two groups, the first at the left and the second at the right side of the ray.

In nodules fixed 25 DAI, serial tangential sections of the proximal part of the NVT showed that regardless of the position of the trace, several cambial strands circumferentially positioned within the root structure and separated with parenchyma "entered" the NVT from both sides of the ray, as shown in two sections selected from a series (Figs. 10, 11; cf. Figs. 6, 9). The individual bundles of the NVT were connected to one side of the ray only. In nodules fixed 60 DAI the NVT consisted of a few groups of trace bundles (Figs. 4, 12), which in the proximal part of the trace had multiple lateral connections to the root secondary xylem (Fig. 13) and multiple circumferential cambial connections with the root cambium (Fig. 14). All these cambial connections in the proximal part of the NVT centrifu-





**Figs. 6–8.** Organization of proximal and middle parts of nodule vascular trace in *Lupinus luteus*, 25 DAI, sections transversal to root axis; trace positioned opposite or laterally to root protoxylem. SPh – secondary phloem; SX – secondary xylem; double arrowheads – cambial strands separated with parenchyma (black stars) connecting root cambium (arrows) and cambial strands within NVT bundles (arrowheads); white stars – radially arranged short tracheary elements in root secondary xylem; double-pointed arrows – pericycle of NVT; white rosettes – NVT phloem; black rosettes – NVT xylem. Bars = 125  $\mu$ m.

gally produced sieve elements and companion cells, with a small number of parenchymatous cells. The strands that remained active for a longer time centripetally produced tracheary elements alternating with parenchyma cells. Serial tangential sections of 25- or 60-day-old nodules showed that the cambial strands present at the time of fixation did not function through the whole cycle of the NVT. Many bundles connecting the NVT with root secondary vascular tissues contained only differentiated cells: some cambial strands must have disappeared. Consequently, in the serial tangential sections the older anastomoses between NVT xylem and root xylem did not match the existing cambial strands. Such cambial activity resulted in the specific structure of the NVT: it was compact in its distal and middle parts, while in the proximal part the trace

diffused into numerous fine strands of tracheary elements interposed with parenchyma (Fig. 9). Characteristically, no functioning phloem was ever left within the part of the NVT inside the layer of root cambium.

The cambial connections allowed the NVT to elongate, mainly through centripetal production of parenchymatous or tracheary elements. Thus the secondary growth of root vascular tissues did not break or overstretch the cells in the proximal part of the trace.

Serial tangential sections showed that the organization of the middle part of the NVT varied between nodules; it could contain either separate groups of bundles separately surrounded by endodermis (Figs. 15, 16) or separate groups of bundles surrounded by a common endodermal layer, or a

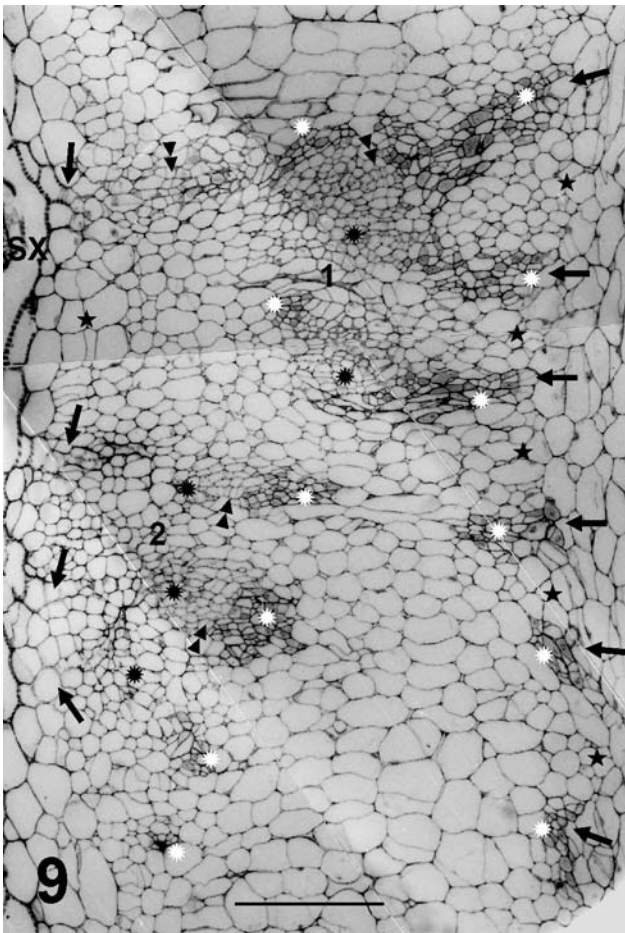
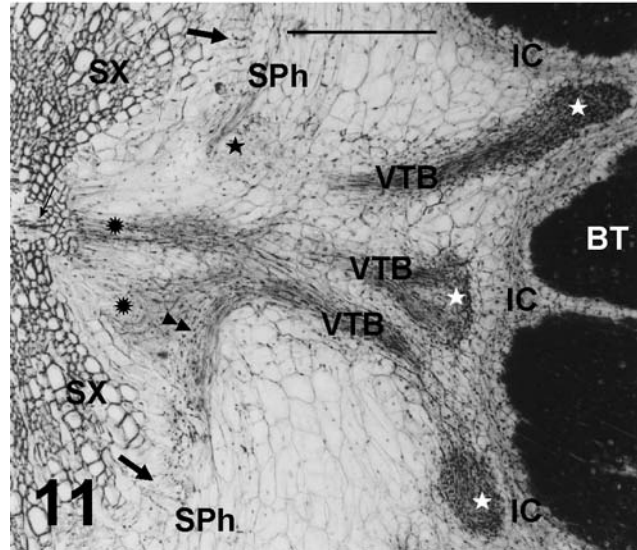
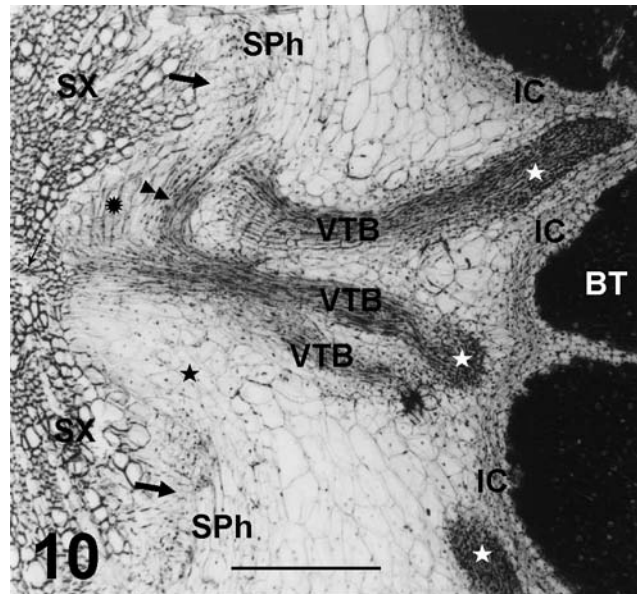


**Fig. 9.** Organization of proximal part of nodule vascular trace in *Lupinus luteus*, 25 DAI, section tangential (approximately) to root axis (secondary xylem is exposed on left side, while phloem is not yet visible on the right). 1-2 – position of two groups of vascular bundles within the NVT as determined from serial sections; SX – secondary xylem; arrows – position of cambial strands (visible only in places indicated with double arrowheads) separated by parenchyma (stars) that connected the trace with root cambium; white rosettes – NVT phloem; black rosettes – NVT xylem. Bar = 125  $\mu$ m.

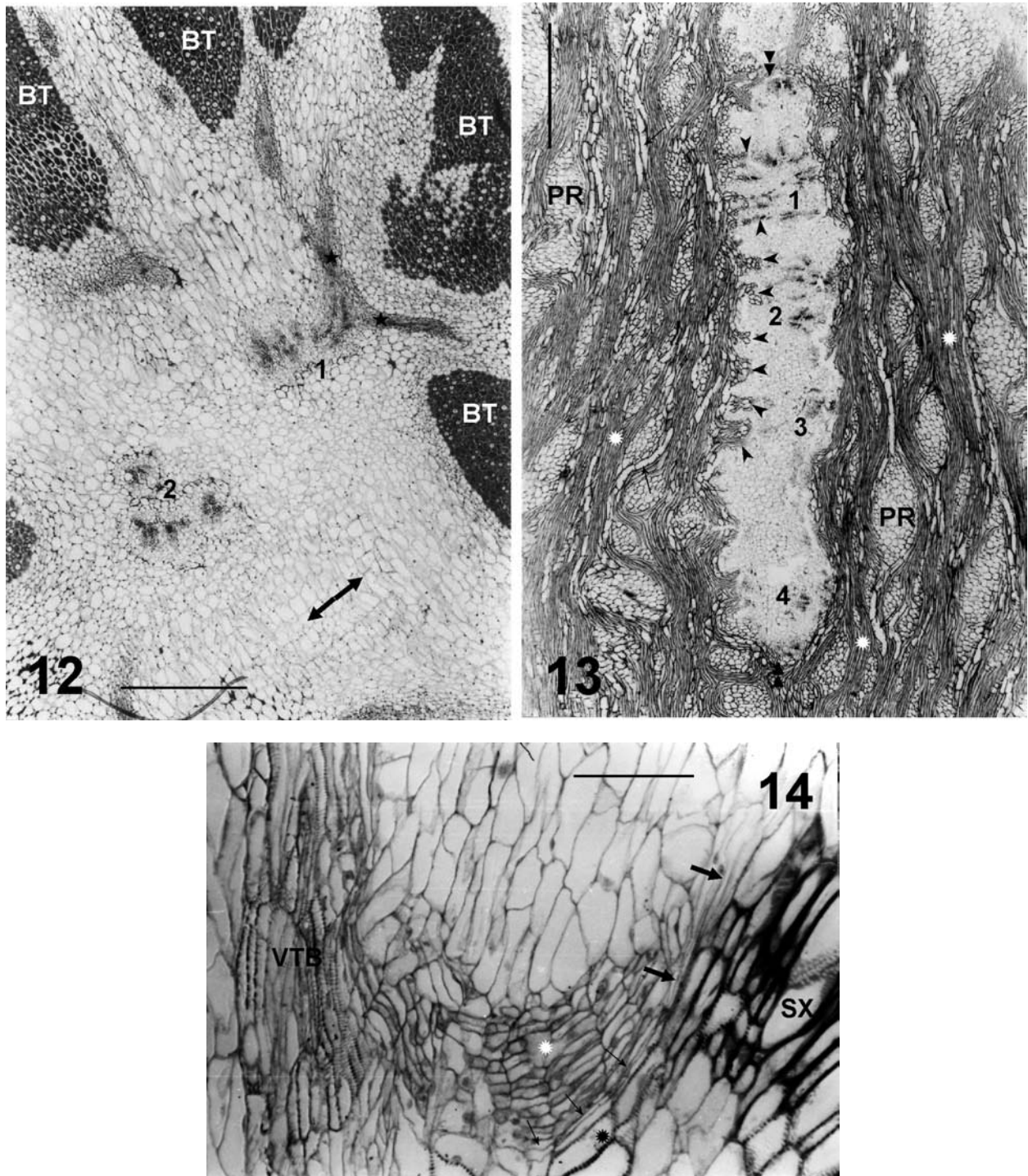
single group of bundles. Inside the NVT endodermis the trace pericycle was uni- or biseriate, composed of vacuolated cells. In cross section (tangential section of nodulated root), NVT phloem was located outside the xylem. In macerated NVT preparations, vessel members were found with a helical secondary wall and simple, often subapical perforation plates, as well as tracheids with a helical secondary wall. In preparations from the proximal part of the trace, small, variously shaped tracheids were found, with helical or reticulate thickenings. In sections, similar elements adjoined the root primary xylem (cf. Part 1 of this work).



**Figs. 10, 11.** Organization of cambial connections in proximal part of nodule vascular trace in *Lupinus luteus*, 25 DAI, sections from the same nodule, transversal to root axis. BT – bacteroid tissue; IC – inner cortex of nodule; SPh – secondary phloem; SX – secondary xylem; VTB – vascular trace bundle; arrows – root cambium; double arrowheads – cambial strands separated by parenchyma (asterisks) connecting NVT with root cambium; rosettes – NVT xylem; white stars – first-order ramifications of NVT bundles in distal part. Bar = 320  $\mu$ m.

The trace bundles in 60-day-old nodules were thicker than in 25-day-old ones. Since some fascicular cambium was visible in NVT bundles in transversal section (Figs. 15, 16), the thickening must have resulted from cell divisions rather than cell enlargement. Indeed, such divisions were occasion-

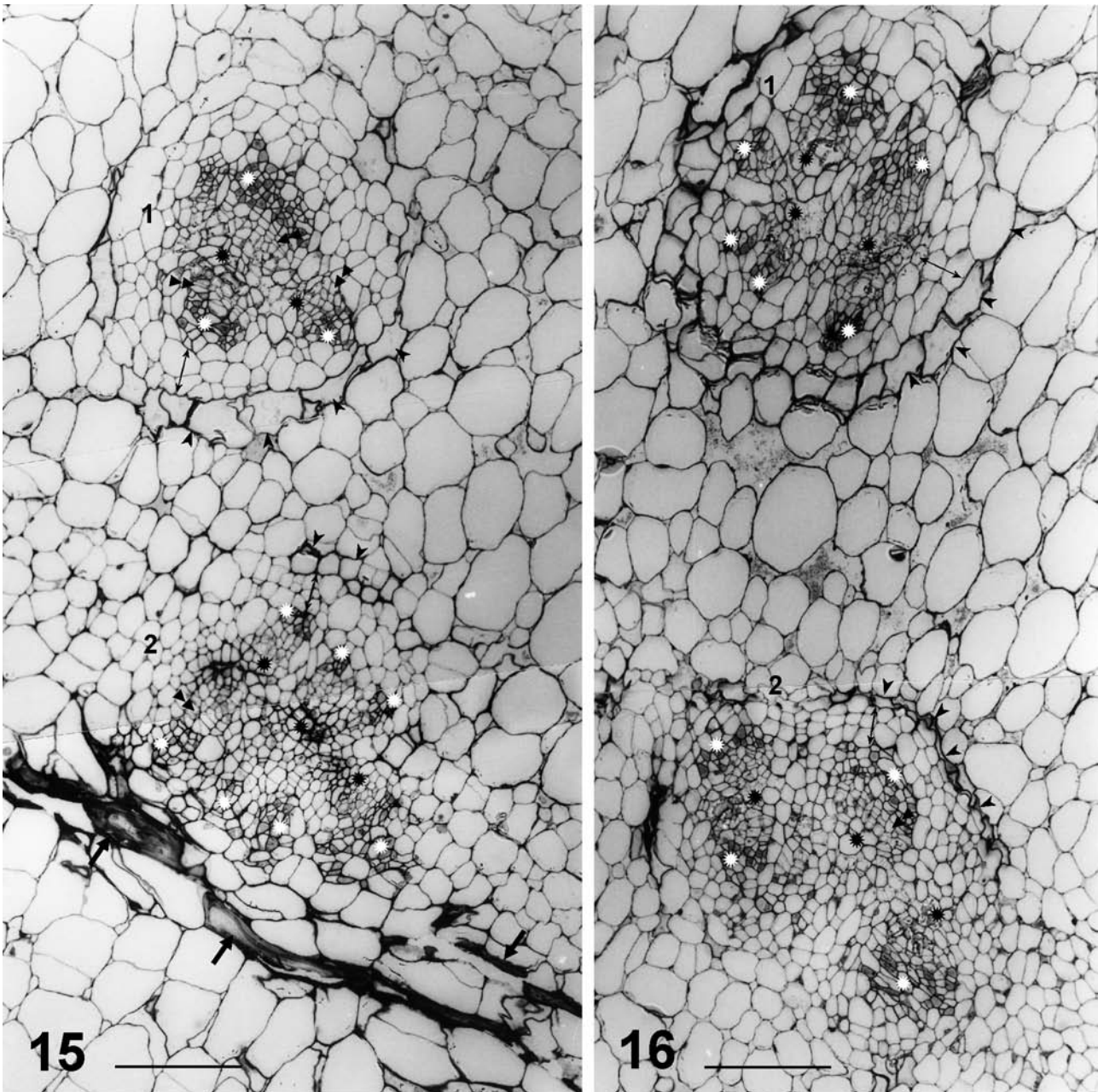




**Figs. 12, 13.** Organization of nodular vascular trace in *Lupinus luteus*, 60 DAI, sections in distal (Fig. 12) and proximal (Fig. 13) parts, transversal root axis. BT – bacteroid tissue; PR – parenchyma ray; double-pointed arrow – axial direction in root; 1, 2 or 1–4 – groups of trace bundles; stars – first-order ramifications of NVT; double arrowheads indicate height of NVT; arrowheads indicate position of lateral connections of NVT with root vascular system; thin arrows – vessels within root secondary xylem; rosettes – xylem fibers. Bars = 830  $\mu\text{m}$  in Fig. 12, 1110  $\mu\text{m}$  in Fig. 13.

**Fig. 14.** Organization of nodular vascular trace in *Lupinus luteus*, 60 DAI, section transversal to root axis. SX – secondary xylem; VTB – NVT bundle; white rosette, thin arrows, black rosette – position of phloem, cambium and xylem, respectively, within lateral connection of NVT and root vascular system; arrows – root cambium (note deeper location of cambial connection in comparison with root cambial cylinder). Bar = 120  $\mu\text{m}$ .





**Figs. 15, 16.** Organization of proximal (Fig. 15) and middle (Fig. 16) part of nodule vascular trace in *Lupinus luteus*, 25 DAI, section tangential (approximately) to root axis (primary phloem fibers are exposed on left side in Fig. 15). 1–2 – position of two groups of vascular bundles versus bundles within the NVT in Fig. 9, as determined from serial sections; arrows – fibers of root primary phloem; white and black rosettes – NVT phloem and xylem, respectively; double arrowheads – NVT fascicular cambium (note that it disappeared from certain bundles); double-pointed arrows – NVT pericycle; arrowheads – NVT endodermis (note that both groups of bundles are separately surrounded by endodermis). Bars = 105  $\mu$ m.

ally seen in sections stained with Mayer's hematoxylin. Regardless of nodule age, in the proximal part of the NVT all the larger bundles contained fascicular cambium (Fig. 15), unlike in its middle or

distal parts, where the meristem disappeared from some bundles (Fig. 16).

In the distal part of the NVT, inversion of the phloem versus the xylem occurred at the site of first-



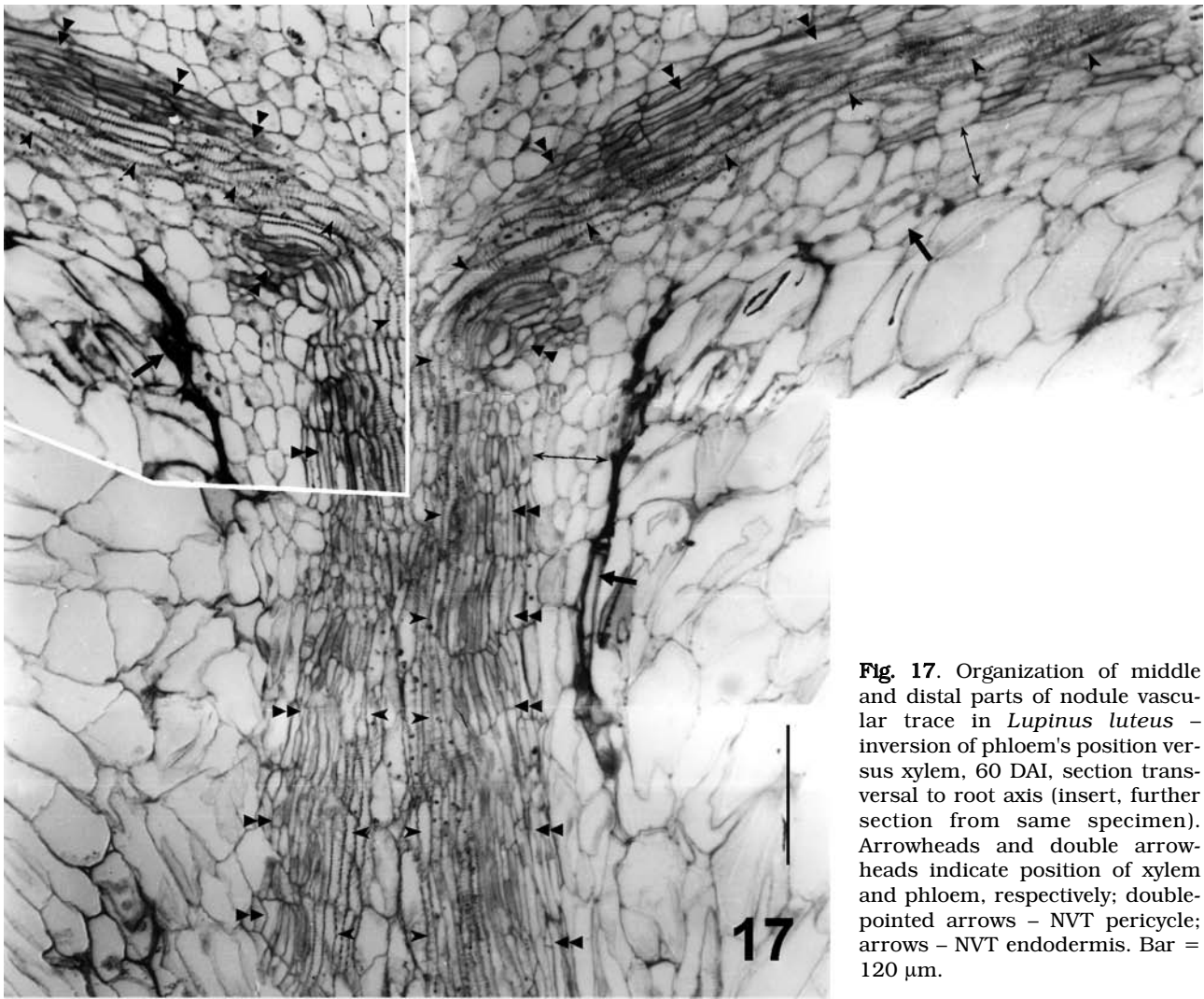


**Fig. 17.** Organization of middle and distal parts of nodule vascular trace in *Lupinus luteus* – inversion of phloem's position versus xylem, 60 DAI, section transversal to root axis (insert, further section from same specimen). Arrowheads and double arrowheads indicate position of xylem and phloem, respectively; double-pointed arrows – NVT pericycle; arrows – NVT endodermis. Bar = 120  $\mu\text{m}$ .

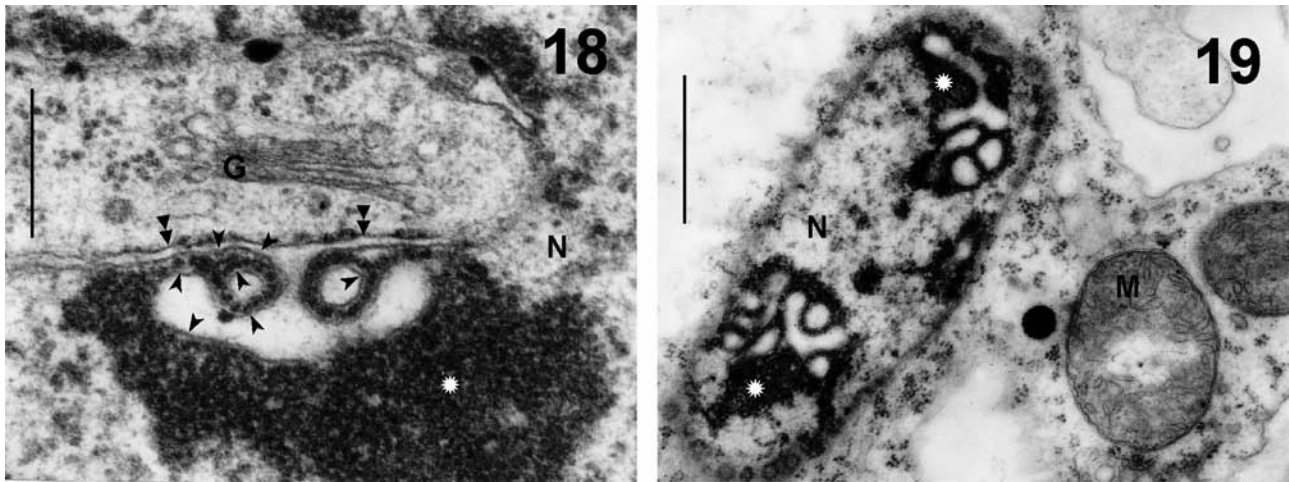
order branching of the trace (Figs. 17). The orientation of the xylem is centrifugal, specific to the NVB.

#### NODULE VASCULAR TRACE – ULTRASTRUCTURE

In the proximal part, most of the volume of the trace was occupied by vacuolated and usually thin-walled parenchyma cells. Xylem-associated transfer cells occasionally occurred in the proximal part. They adjoined tracheary elements of the NVT or vessel members of root secondary xylem. The wall ingrowths were small and limited to the wall adjoining the tracheary element. In NVTs of 25-day-old nodules, the primary cell wall of the oldest tracheary elements degraded until only electron-dense fibrils were left. The number of nonfunctional, obliterated tracheary elements increased in nodules fixed 60 DAI; such elements also became visible by LM. At the same time, differentiating tracheary elements

that still contained the protoplast occurred closer to the NVT fascicular cambium. In the middle and distal part of the NVT, parenchyma cells adjoining tracheary elements were sporadically specialized as transfer cells rich in mitochondria and multivesicular bodies.

In the trace's proximal part, nonfunctional phloem was present in 25-day-old nodules; thick callosic deposits blocked the sieve plates in the oldest sieve elements. As a rule, NVT companion cells formed small ingrowths on their whole wall, regardless of nodule age. In younger phloem, the companion cells' protoplast was not vacuolated. In older phloem, vacuolation occurred and the mitochondria became enlarged and electron-transparent. An electron-dense substance accumulated within the companion cells' cytoplasm and vacuoles, and eventually the companion cell degraded and disintegrated together with the sieve tube. Degraded companion



**Figs. 18, 19.** Ultrastructure of vascular trace in *Lupinus luteus* root nodules, 25 DAI, nuclei in pericycle of middle and distal trace. G – Golgi apparatus; M – mitochondria; N – nucleus; arrowheads – nuclear envelope's inner membrane; double arrowheads – nuclear envelope's outer membrane; rosettes – dense chromatin. Bars = 0.4  $\mu$ m in Fig. 18, 1.0  $\mu$ m in Fig. 19.

cells were rare in 25-day-old nodules, frequent in 60-day-old ones, but young (differentiating) phloem cells were always seen in the same sections, due to the sustained mitotic activity of cambial cells. The phloem or xylem fibers typical of root vascular tissues were never found in any part of the NVT.

The pericycle cells of the middle and distal parts of the NVT were vacuolated and devoid of wall labyrinth. In material fixed 25 DAI (but not 60 DAI), their lobed nuclei developed an especially distinct and extensive system of invaginations of the nuclear envelope's inner membrane (Figs. 18, 19), which enlarged the perinuclear space. Within the invagination lumen, fine-fibrillar content was often observed. The invaginations were located exclusively within dense chromatin, including nucleolar chromatin. There were some invaginations within the chromatin that were not connected with the inner membrane. Judging from the appearance of the invaginations in surface-sectioned nuclei (Fig. 19), the disproportion resulted from branching and coiling of the particular invagination. Such a transformation of the nuclear envelope ultrastructure was also observed in pericyclic transfer cells of NVBs (and in the proximal part of of NVTs of juvenile nodules; cf. Part 1 of this work).

#### STRUCTURE OF NODULE VASCULAR BUNDLES

In cross-section, endodermis-ensheathed NVBs contained the pericycle (uniseriate in younger parts of bundles and 2–3-layered in older ones), xylem and phloem. Various orientations of cell divisions were often observed within the pericycle, and divisions also occurred in cells already differentiated, including transfer cells. Divisions were also observed within

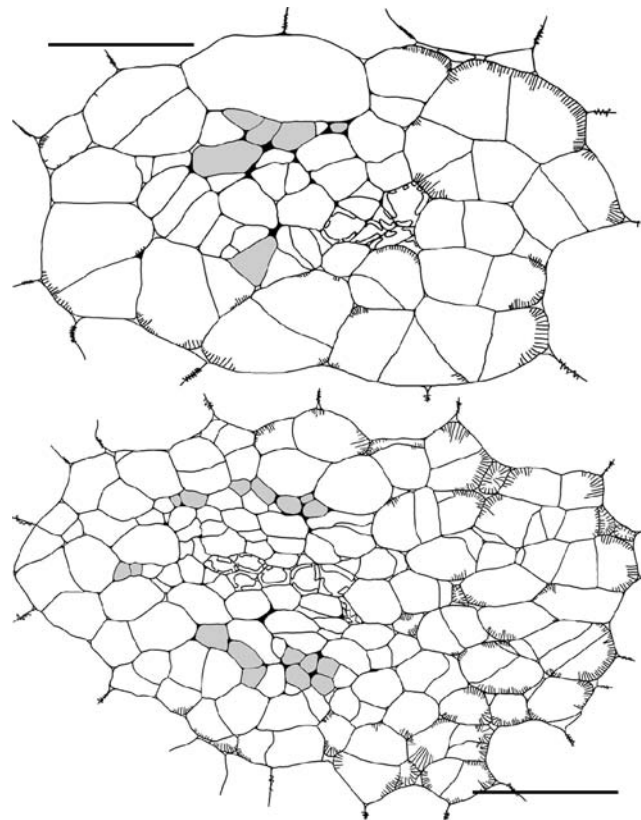


**Fig. 20.** Structure of vascular bundles in *Lupinus luteus* root nodule, 25 DAI. Upper bundle sectioned close to its apex, lower bundle close to its base. Cells with irregularly thickened walls – tracheary elements; grey – sieve tubes; bars – wall labyrinth of transfer cells. Note that in lower bundle, which was positioned between lobes of bacteroid tissue, xylem is half-encircled with phloem. E – NVB endodermis; P – NVB pericycle. Bars = 15  $\mu$ m in upper and 33  $\mu$ m in lower drawing.



TABLE 1. Structure of the NVBs of 25 day-old root nodules of *Lupinus luteus* L.

Element type	Number of elements in bundle no.:								Average
	1	2	3	4	5	6	7	8	
Total number of cells	55	64	71	84	92	174	186	189	114
Tracheary elements	4	3	6	5	8	7	8	14	7
Sieve elements	5	7	7	6	8	15	12	17	10
Parenchyma cells	46	54	58	73	76	152	166	158	97
Transfer cells	22	31	25	18	17	43	53	48	32
Adjoining endodermis	13	16	16	8	9	27	21	25	17
Middle-positioned	2	11	4	3	6	16	30	18	11
Adjoining tracheary elements	7	4	5	7	2	0	2	5	4
Number of parenchyma cells with nuclei visible in section	17	10	22	14	18	46	42	48	27
cells with invaginations of the nuclear envelope's inner membrane	13	9	16	3	4	35	15	37	17
Number of transfer cells with nuclei visible in section	10	7	15	5	3	19	17	17	12
transfer cells with invaginations of the nuclear envelope's inner membrane	10	7	14	2	3	18	14	15	10

the bundle's fascicular cambium, and the daughter cells usually differentiated as phloem elements.

The NVB pericycle cells were axially elongated and larger than the vascular parenchyma cells located deeper in the bundle. In pericycle cells the nucleus was usually irregular but not lobed, unlike in the NVT pericycle. Within the dense chromatin, invaginations of the envelope's inner membrane were observed, less extensive than in the NVT of the same nodule. The cell wall was thin, with numerous plasmodesmata connecting the cell with other NVB cells or endodermis. Wall ingrowths were formed in numerous pericyclic cells. The wall labyrinth was most elaborate on the endodermis-adjointing wall, close to walls anticlinal to the endodermis and on anticlinal walls of deeper-located cells (Fig. 20). Pericyclic transfer cells were usually completely absent from the phloem-adjoint area.

Phloem and xylem were arranged collaterally, with the phloem facing bacteroid tissue. In bundles positioned between lobes of bacteroid tissue (i.e., with bacteroid tissue present at two or three sides of the bundle), the xylem was surrounded by a semi-circle of phloem (Fig. 20). No phloem or xylem fibers were ever found in NVBs. Vessel members and tracheids, both with helical thickenings, were found in macerated preparations of nodule bundles. Adjoining parenchymatous cells developed a moderately elaborate wall labyrinth, usually on the wall facing the tracheary element. Within the bundle it was often impossible to distinguish phloem and xylem parenchyma, as all the inner parenchymatous cells were ultrastructurally similar and adjoined

both tracheary and sieve elements. In NVBs the companion cells lacked wall ingrowths.

In 60-day-old nodules, symptoms of degradation were observed in NVB phloem, tracheary elements and pericycle, especially in first-order bundles. At the same time, in younger parts of NVBs the cells exhibited ultrastructural traits of intensive metabolic activity: many mitochondria with expanded cristae, many RER cisterns and Golgi bodies.

The frequency of particular elements of NVBs (Tab. 1) was calculated using low magnification (up to 3200 $\times$ ) serial electronograms mounted together. The calculation is approximate only, as costs limited our mapping to only eight randomly chosen bundles. Tracheary elements comprised 6% of the total number of cells, sieve tubes 9%, and parenchyma cells 85%; 33% of all parenchyma cells were specialized as transfer cells. The majority of transfer cells (54%) adjoined bundle endodermis, ~30% were located deeper within the bundle, and ~16% of the transfer cells adjoined tracheary elements. Normally the nucleus was visible in ~27 parenchyma cells per bundle section, and up to 59% of these nuclei formed invaginations of the nuclear envelope's inner membrane. The share of transfer cells in this group (taken as 100%) reached 71%. Taking the average number of transfer cells with the nucleus visible in section as 100%, 83% of the transfer cells developed invaginations of the nuclear envelope's inner membrane. On the basis of cell counts and general observations, it is reasonable to suggest that this trait is specific to this group of cells.

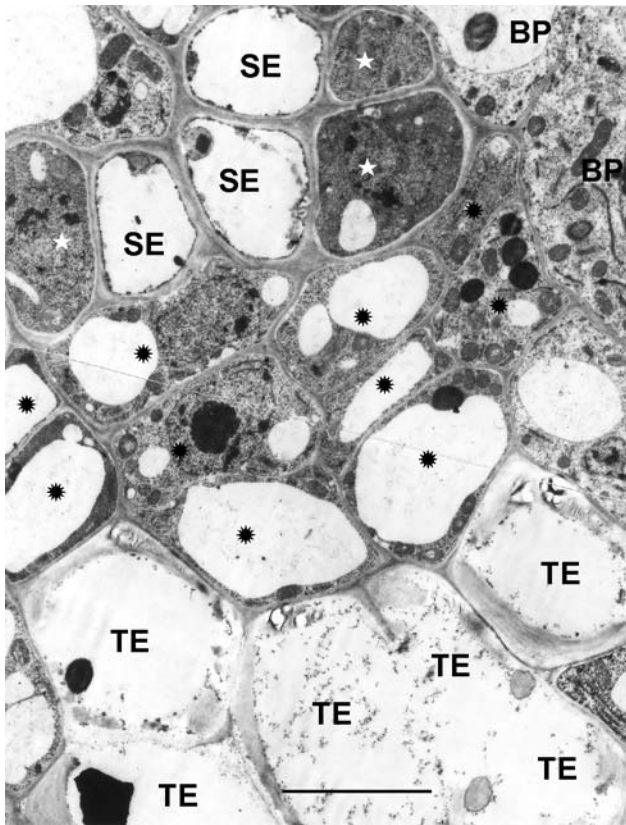


**Fig. 21.** Organization of nodule bundles in *Lupinus luteus* – linear arrangement of cells between bundle xylem and phloem, 60 DAI. BP – vascular bundle parenchyma; SE – sieve element; TE – tracheary element; stars – companion cells; rosettes – putative fascicular cambium cells in linear arrangement. Bar = 4.0  $\mu\text{m}$ .

The spatial system of NVBs was much expanded in 60-day-old root nodules, corresponding to the remarkable growth of the whole nodule. Close to the differentiated bacteroid tissue and especially between the lobes of the tissue, the bundle apices were completely differentiated and encircled by endodermis. Serial tangential sections showed that the differentiated apices were 10–60  $\mu\text{m}$  long, and usually they were third- or fourth-order ramifications. In the bundle in cross section,  $\sim 10$  parenchymatous cells occurred at the differentiated apices, together with 4–20 sieve elements and 2–10 tracheary elements. In some apices only sieve elements were observed. In the central part of some older (and thicker) bundles, xylem and phloem elements were arranged linearly (Fig. 21), indicating activity of fascicular cambium, at least temporarily maintained. NVB apices positioned at younger bacteroid tissue, and especially at its meristematic parts, comprised only non-differentiating cells.

Serial tangential sections revealed the interrelationship of the development of nodule bundles and

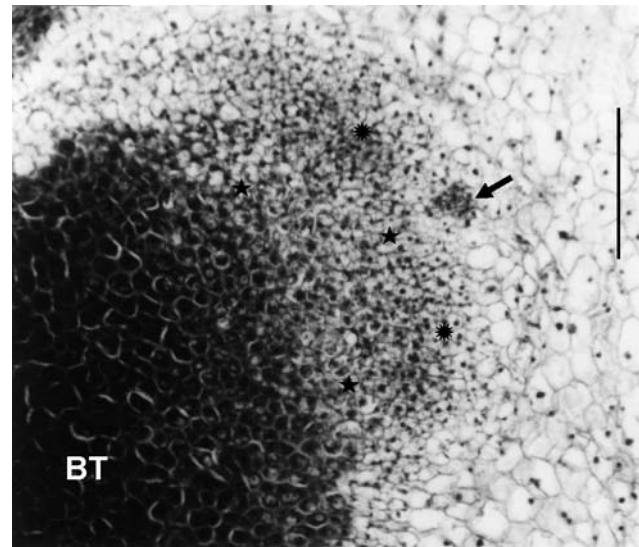


**Fig. 22.** Coordinated development of nodule bundles and meristems in *Lupinus luteus* root nodule, 60 DAI. BT – bacteroid tissue; arrow – NVB apex; rosettes – meristems flanking bundle apex; stars – differentiating bacteroid tissue. Bar = 170  $\mu\text{m}$ .

nodule meristems. If an NVB apex was present at the front of the meristem, the nearest meristematic cells exhibited traits of differentiating bacteroid cells rather than meristematic ones (Fig. 22), and thus the truly meristematic tissue was divided into two parts flanking the differentiating bundle apex. A bundle developing autonomously, independently of the nodule meristem, for example on the basis of cell dedifferentiation at the front of the bundle apex, was never observed. However, some intercalary growth of the bundle resulted due to the observed transversal (versus the bundle axis) divisions of some bundle cells, and together with cell elongation it probably balanced the expansion of neighboring bacteroid tissue. At the same time, the bundle apex elongated due to the mitotic activity of non-infected nodule meristem cells.

## DISCUSSION

### VASCULAR TISSUE IN ROOT NODULE VERSUS ROOT AND LEAF

In vascular tissues of root nodule and leaf, physiological similarities that might result in their structural resemblance are recognized (Pate et al., 1969). Both organs assimilate a crucial nutrient, both export the bulk of their production via a network of vascular bundles, and both organs are strong sinks of substances from another organs. In yellow lupine, however, the vascular tissue of the root nodule



described in this work is distinct from that of root or leaf (all data on yellow lupine root or leaf vascular tissues are the author's unpublished observations). Anatomical differences obviously result from differences in the organization of vascular meristems, but the vascular tissues of the root, root nodule and leaf differ ultrastructurally as well. In the lupine nodule, no cells specialized in mechanical function are ever formed, while such cells are abundant in root secondary xylem and protophloem. The differences between types of vascular parenchyma cells (VPCs) seem most significant. Many nodule VPCs develop invaginations of the nuclear envelope's inner membrane. Such cells do not occur in the root or leaf of *L. luteus*. In the root, only companion cells specialize as transfer cells, while the nodule vascular system is characterized by a specific pattern of transfer cell location that changes in time.

The leaf veins are more variable than NVBs as to their area and cell number in cross section. While the thickest nodule bundles and the first-order veins of leaves have a similar total number of cells (~180) in cross section, the apices of nodule bundles consist of ~50 cells, versus not more than 20 cells for leaf vein endings.

The leaf veins and NVBs are distinct with regard to the location of transfer cells and the structure of their wall labyrinth. The transfer cells differentiate at sites of intensive solute exchange at the apoplast/symplast interface (Gunning and Pate, 1969; Pate and Gunning, 1972). They are specialized for short-distance active transport of solutes, with increased plasma membrane area and correspondingly more membrane-bound transporters. In lupine leaf vein endings, 100% of the vascular parenchyma cells, including companion cells, transform into transfer cells, while in the NVB apices only ~33% do, and the NVB companion cells have no wall labyrinth; the pericycle cells (absent from leaf veins) specialize as transfer cells. In lupine root nodules, NVB pericyclic transfer cells load the NVB apoplasts with  $N_2$  fixation products (amides in lupine), which thereafter are exported from the nodule via tracheary elements (Gunning and Pate, 1969; Pate and Gunning, 1972). The absence of wall labyrinth in companion cells of lupine NVBs (this work) imply symplastic unloading of sieve tubes and further symplastic transport of imported solutes to bacteroid tissue. Plasmodesmata, needed for such a transport pathway, are abundant along this pathway (author's observations). What is the role of the transfer cells that differentiate within the lupine NVT? If, as according to Pate (1986), the connection of the nodule and root vascular system is considered to be the equivalent of the stem's node, then solute transfer between phloem and xylem may be a function of transfer cells in the proximal part of the NVT.

The spatial arrangement of bacteroid and vascular tissue of the root nodules seems to be less adapted to effective exchange of condensed solutes between tissues than the complex venation in leaf mesophyll (Pate et al., 1969). The surface area of NVBs is just a few percent of the surface area of the nodule section (Pate et al., 1969; Łotocka et al., 1995), and the solutes exported from the bacteroid cells traverse a distance of 0.3–1.3 mm to reach the vascular tissue (Pate et al., 1969). The maximum distances between leaf mesophyll cells and vein endings are usually much shorter (Esau, 1967). However, the considerable distance to be crossed by exported  $N_2$  fixation products is not significant to the efficiency of export from root nodules: nitrogen fixation was never observed to become limited by its accumulated products, that is, by insufficiently intensive export. That implies that NVB apoplast loading by transfer cells is highly efficient and reliable.

#### NUCLEAR ENVELOPE

The ultrastructure of cell nuclei, with the invaginations of the envelope's inner membrane presently observed in lupine nodule vascular parenchyma, suggests similarities with the nuclear vacuoles, for example in tapetal cells or the developing male gametophyte of *Gossypium hirsutum* or *Populus simonii* (Wang et al., 1994), or meiotic prophase in *Beta vulgaris*, *Olea europaea*, *Pteridium*, *Dryopteris*, *Marsilea*, *Pinus* and *Lycopersicon* (Rodriguez-Garcia et al., 1988; Sheffield et al., 1979). However, none of the published images resemble the invaginations associated exclusively with dense chromatin observed in the lupine NVT pericycle or in NVB transfer cells. Also different is the location of nuclei within the plant body (sporogenous tissue/vascular tissue), or within the cell cycle (meiotic division/differentiated stage). Several alternative explanations of the formation or role of the nuclear vacuole have been proposed (Rodriguez-Garcia et al., 1988; Sheffield et al., 1979), and no experiments have been done to test the possibilities. None of the data presented here permit a clear hypothesis on the function of the invaginations observed in lupine. They definitely are not degenerative, as they appear during the very first stages of nodule vascular system ontogenesis, and then in young cells and in transfer cells, characterized by high metabolic activity.

#### VASCULAR SYSTEMS IN LUPINOID VERSUS CYLINDRICAL ROOT NODULES – GENERAL DISCUSSION TO PARTS 1 AND 2

This discussion compares lupine with clover, since the latter's root nodule vascular system is relatively well-explored. If not indicated otherwise, the data on

clover originate from the author's unpublished observations.

The root nodules of clover and lupine are of indeterminate type, that is, their growth relies on continuous meristematic activity. In clover, however, the connection between root and nodule is formed without the participation of endodermis derivatives in the process (Łotocka et al., 1997). The connection – a single collateral vascular bundle – bifurcates at the oldest part of the bacteroid tissue, and every branching soon forks again. The resulting nodule vascular system contains no more than 20 meristematic bundle apices in 42-day-old clover nodules, much less than in lupine nodules of similar age. The difference results from the relative sizes of clover and lupine nodules, since in both plants the vascular tissue corresponds to ~2% of total nodule volume (Roughley, 1970; Łotocka et al., 1995).

An apparently much more significant difference concerns the mode of expansion of the vascular connection between the root and nodule. In clover, as mentioned, the connection is a single vascular bundle (Łotocka et al., 1997). The nodule proximal bundle (vascular connection) contains fascicular cambium, which is a fold-like extension of root cambium. In serial sections of clover nodulated root, the proximal bundle fuses smoothly with secondary root tissues until cambia and vascular tissues are completely integrated. The proximal bundle extends from the root at a small angle, which poses no obstacle to matching up the secondary growth of root vascular tissues to the thickening of the proximal bundle. Unlike in clover, in lupine the vascular connection between root and nodule (nodule vascular trace) stands distinctly apart from the root secondary tissues, on both anatomical and ultrastructural levels. In lupine the NVT is perpendicular to the root stele, and thus its proximal part is subjected to tension due to root xylem secondary growth, which in lupine is much more intensive than in clover. In clover, unlike in lupine, the derivatives of proximal bundle cambium differentiate into root-like vascular tissues: up to 10 phloem fibers are formed in the proximal bundle, the VPCs are identical with those located in roots, and the transfer cell pattern is the same as in roots. In both species there are transfer cells adjoining the tracheary elements, and the companion cells within the vascular connection with the root are specialized as transfer cells, ultrastructurally identical to those in root.

In the meristematic distal part of lupine NVT, the cells are positioned within a different phytohormone gradient than in the proximal part, since the bacteroid tissue can be a source of phytohormones (lupine: Dullaart, 1970; reviews: Franssen et al., 1992; Hirsch and Fang, 1994). This could result in reversion of the transversal polarity of the fascicular cambium in distal NVTs and consequently in inversion of the position of phloem versus xylem. In clover

there is no need for the reversal of the relative positions of phloem and xylem observed in lupine, since in clover the phloem is already properly oriented (towards the bacteroid tissue) in the proximal bundle.

The general structure of NVBs is similar in the two species, with some exceptions concerning the frequency and location of wall ingrowths in transfer cells (Pate et al., 1969). The presence of parenchymatous cells with invaginations of the nuclear envelope's inner membrane is unique to lupine. Apart from the meristematic apices, neither dividing cells nor a linear cell arrangement (suggesting the activity of fascicular cambium) are observed in clover NVBs, unlike in lupine. In clover every bundle apex is meristematic, while in lupine many apices situated at differentiated bacteroid tissue are completely differentiated. The meristematic apices of NVBs merge with the nodule meristem in both species. In clover, the apical nodule meristem consists exclusively of rhizobia-free cells (Łotocka et al., 1997). In lupine the multiple lateral nodule meristems consist of two cell types, and the rhizobia-free cells that produce cortical tissues also elongate the NVBs. The possibility of discrete initials of bundles remains to be examined in both species.

To the best of my knowledge this is the first comprehensive report on the developmental anatomy of the root nodule vascular system involving the initial stages of nodule formation. In lupine the course of nodule vascular system ontogenesis and the differences in cell ultrastructure in its different parts suggest that initially the development of nodule vascular tissues might be controlled by root-borne factors, and that later control is taken over by nodule meristems to coordinate the formation of bacteroid and vascular tissues. The unique traits of vascular differentiation in yellow lupine nodule are (i) the formation of the NVT as a distinct part of the system and (ii) the specific structure of the proximal part of the NVT, enabling concerted growth of the root and nodule. Ultrastructural changes in the vascular parenchyma were described here for the first time; they consist in the formation of invaginations of the nuclear envelope's inner membrane, associated with dense chromatin.

## ACKNOWLEDGEMENTS

I thank Dr. Ewa Kurczyńska for helpful comments on the manuscript, and Ewa Znojek and Alicja Żuchowska for expert technical assistance.

## REFERENCES

- BRIARTY LG. 1978. The development of root nodule xylem transfer cells in *Trifolium repens*. *Journal of Experimental Botany* 29: 735–747.



- BRODA B. 1971. *Metody histochemii roślinnej*. PZWIL, Warsaw.
- DULLAART J. 1970. The bioproduction of indole-3-acetic acid and related compounds in root nodules and roots of *Lupinus luteus* L. and by its rhizobial symbiont. *Acta Botanica Neerlandica* 19: 573–615.
- ESAU K. 1967. Minor veins in *Beta* leaves: structure related to function. *Proceedings of the American Philosophical Society* 111: 219–233.
- FRANSSEN HJ, HORVATH B, LADOS M, VAN DE VIEL C, SCHERES B, SPAINK HP, and BISSELING T. 1992. Nodule formation and hormone balance. In: Karssen CM, Loon van LC, and Vreugdenhil D [ed.], *Progress in plant growth regulation*, 522–529. Kluwer Academic Publishers.
- GERLACH D. 1972. *Zarys mikrotechniki botanicznej*. Państwowe Wydawnictwo Rolnicze i Leśne, Warszawa.
- GUNNING BES and PATE JS. 1969. "Transfer cells". Plant cells with wall ingrowths, specialized in relation to short distance transport of solutes – their occurrence, structure and development. *Protoplasma* 68: 107–133.
- HIRSCH AM. 1992. Developmental biology of legume nodulation. *New Phytologist* 122: 211–237.
- HIRSCH AM, and FANG Y. 1994. Plant hormones and nodulation: what's the connection? *Plant Molecular Biology* 26: 5–9.
- ŁOTOCKA B, ARCISZEWSKA-KOZUBOWSKA B, DĄBROWSKA K, and GOLINOWSKI W. 1995. Growth analysis of root nodules in yellow lupin. *Annals of Warsaw Agricultural University – SGGW, Agriculture* 29: 3–12.
- ŁOTOCKA B, KOPCIŃSKA J, BORUCKI W, STĘPKOWSKI T, ŚWIDERSKA A, GOLINOWSKI W, and LEGOCKI AB. 2000a. The effects of mutations in *nolL* and *nodZ* genes of *Bradyrhizobium* sp. WM9 (*Lupinus*) upon root nodule ultrastructure in *Lupinus luteus* L. *Acta Biologica Cracoviensia Series Botanica* 42: 155–163.
- ŁOTOCKA B, KOPCIŃSKA J, and GOLINOWSKI W. 1997. Morphogenesis of root nodules in white clover. I. Effective root nodules induced by the wild type of *Rhizobium leguminosarum* biovar. *trifolii*. *Acta Societatis Botanicorum Poloniae* 66: 273–292.
- ŁOTOCKA B, KOPCIŃSKA J, GÓRECKA M, and GOLINOWSKI W. 2000b. Formation and abortion of root nodule primordia in *Lupinus luteus* L. *Acta Biologica Cracoviensia Series Botanica* 42: 87–102.
- PATE JS, and GUNNING BES. 1972. Transfer cells. *Annual Review of Plant Physiology* 23: 173–196.
- PATE JS, GUNNING BES, and BRIARTY LG. 1969. Ultrastructure and functioning of the transport system of the leguminous root nodule. *Planta* 85: 11–34.
- RODRIGUEZ-GARCIA MI, MAJEWSKA-SAWKA A, and FERNANDEZ MC. 1988. Why do nuclear vacuoles appear in the prophase nucleus of pollen mother cells? Facts and hypotheses. In: Cresti M, Gori P, and Pacini E [ed.], *Sexual reproduction in higher plants*, 163–168. Springer-Verlag, Berlin, Heidelberg, New York, London, Paris, Tokyo.
- ROUGHLEY RJ. 1970. The influence of root temperature, *Rhizobium* strain and host selection on the structure and nitrogen-fixing efficiency of the root nodules of *Trifolium subterraneum*. *Annals of Botany* 34: 631–646.
- SHEFFIELD E, CAWOOD AH, BELL PR, and DICKINSON HG. 1979. The development of nuclear vacuoles during meiosis in plants. *Planta* 146: 597–601.
- WANG Y, YANG S-J, LI M-Y, and LOU C-H. 1994. Nuclear invagination and nuclear vacuole formation in several plants. *Acta Botanica Sinica* 36: 963–966.